Monatsh Chem 139, 319–328 (2008)
DOI 10.1007/s00706-007-0803-2
Printed in The Netherlands

Monatshefte für Chemie
Chemical Monthly

Quantum chemical calculations of electronically excited states: formamide, its protonated form and alkali cation complexes as case studies

Ivana Antol[1], Mario Barbatti[2], Mirjana Eckert-Maksić[1,*], Hans Lischka[2,*]

[1] Division of Organic Chemistry and Biochemistry, Rudjer Bošković Institute, Zagreb, Croatia
[2] Institute for Theoretical Chemistry, University of Vienna, Vienna, Austria

Received 13 August 2007; Accepted 10 September 2007; Published online 14 March 2008

Abstract The properties of formamide, its protonated form and interaction complexes with lithium and sodium cations were studied in electronically excited singlet states by means of high-level multireference *ab initio* methods. The vertical excitation energies show a marked influence on protonation with particular large effects found for the O-protonated form as compared to neutral formamide. Complexation with Li^+ and Na^+ leads to a pronounced shift of the n_O–π^* state to higher energies while the π–π^* state moves in opposite direction. Geometry optimizations in the lowest excited singlet show strong geometrical effects leading to pyramidalization at the N and C atoms. The photodynamical simulations performed for formamide in the first excited singlet state show that the main primary deactivation path is CN dissociation with a lifetime of about 420 fs.

Keywords Photochemistry; Basicity; Absorption; Metal ion affinities; Multireference configuration interaction.

Introduction

It is well known that molecular photoexcitation can lead to dramatic effects in both the molecular structure and the chemical reactivity of a molecule. The underlying cause of this behavior lies in the redistribution of the electronic density following excitation. A particularly fascinating aspect of molecular photoexcitation is the strong change that can occur in acid-base properties. The acidity or basicity of certain functional groups can be either increased or decreased in their excited states [1]. Hence, detailed knowledge about the involved excited states is a prerequisite for a better understanding, for example of photoinduced proton transfer processes in molecular systems. Excited-state intramolecular proton transfer occurs in a large variety of chemical and biological systems and has been investigated very thoroughly by various spectroscopic techniques (see *e.g.*, Ref. [2]), as well as by computational methods [3]. In recent years we have been concerned with exploring the effect of photoexcitation on the basicity of two paradigmatic molecules, namely formaldehyde and formamide using extended quantum chemical methods (multireference configuration interaction (MRCI)) [4, 5]. This interest is connected to the fact that formaldehyde is a prototype model compound where the properties of the carbonyl chromophore can be studied in detail, while formamide presents the simplest amide containing a prototype HNC=O peptide linkage, the moiety that holds amino acid units in polypetides and proteins together. The electronic absorption spectra of both molecules have been measured by several groups, but their assign-

*Correspondence: Mirjana Eckert-Maksić, Division of Organic Chemistry and Biochemistry, Rudjer Bošković Institute, P.O.B. 180, HR-10002 Zagreb, Croatia. E-mail: mmaksic@emma.irb.hr; Hans Lischka, Institute for Theoretical Chemistry, University of Vienna, Währingerstrasse 17, A-1090 Vienna, Austria. E-mail: hans.lischka@univie.ac.at

ment and location of the vertical transitions are by no means unambigous due to the strong mixing of some of the valence excited states with the *Rydberg* states [6, 7]. It is thus not surprising that numerous theoretical studies performed at different levels of theory have been extensively used to aid the assignment of the measured spectra. We mention only the pioneering investigations by *Whitten* and *Hackmeyer* [8], *Buenker* and *Peyerinhoff* [9] and *Basch et al.* [10] as well as more recent complete-active space perturbation theory to second order (CASPT2) [11, 12] and equation-of-motion (EOM) calculations [13, 14]. Particularly significant advances in this area were obtained in recent years owing to the availability of powerful multireference (MR) methods [15–18] which enable the balanced description of valence and *Rydberg* states.

Here we present an overview of the most salient results obtained in our previous studies, together with the preliminary results of some ongoing research in this field. Along the paper, several aspects of Quantum Chemistry applied to the calculation of excited states will be highlighted. From the accurate calculation of excited-state energies and the characterization of electronic wavefunctions of excited states until the determination of excited-state optimized structures and conical intersections, this kind of investigation is not only computationally demanding, but also covers a wide range of quantum chemical methods beyond the standard single-reference approaches applicable for ground-state structures in the neighborhood of the energy minimum. The already mentioned advance in MRCI techniques is based on the development of the COLUMBUS program system [19] where recent progress has been made by the development of procedures for the computation of analytical gradients and analytical nonadiabadic coupling vectors at MRCI and multiconfiguration self-consistent field (MCSCF) levels [20], which allow the efficient optimization of geometries strongly distorted with respect to ground-state structures that often appear during excited-state relaxation. In a next significant step, the availability of these quantities has led to the development of the program system NEWTON-X [21] to be used for nonadiabatic excited-state dynamics simulations at multireference *ab initio* levels. The combination of the two program systems and the computational methods involved in them has opened new possibilities for the detailed simulation of primary photochemical processes and allows a deepened insight into their mechanistic and dynamical aspects.

In the first part of the paper we shall discuss results of multireference configuration interaction with singles and doubles plus Davidson corrections (MR-CISD + Q) calculations of UV absorption spectra of formamide and its protonated forms [5]. A comparison to the corresponding spectra of formaldehyde and its protonated form will be given also [4]. This discussion will be followed by a description of the calculated UV spectra of Li^+ and Na^+ ion complexes with formamide [22]. The latter cases are of considerable interest due to the fact that contrary to the case of the protonated species the cation-oxygen bond in metal ion complexes is predominantly electrostatic in nature. Hence, smaller shifts of the n_O–π^* and π–π^* excited states in these complexes are expected in comparison to protonation [23]. In the second part of this work the effect of molecular photoexcitation on proton affinities of formaldehyde and formamide will be considered in detail. This will be followed by a brief survey of our preliminary results obtained in a computational study of the lithium cation and sodium cation affinities of formamide in the ground and in the first excited singlet state [22]. The gas-phase complexation of the peptide bond with metal ions is highly relevant from the biological point of view since it can provide a deeper insight into the intrinsic interactions between metal ions and biomolecules involved in biochemical reactions governing the cation exchange at cellular level. In addition, this type of cations is also of considerable importance as a tool for investigating the amino acid sequence of peptides. The photochemistry of formamide, including the results of our recently-performed excited-state dynamics simulations will be discussed in the last part of the paper.

Results and discussion

Ground state geometries

An overview of the ground state geometries of the species discussed in this work is presented in Fig. 1 [5] in order to facilitate the discussion of structural changes upon protonation or metal association. It should be noted that in the metal ion complexes only the structure with the metal cation associated with the oxygen atom represented an energy minimum in accordance with previously published results of

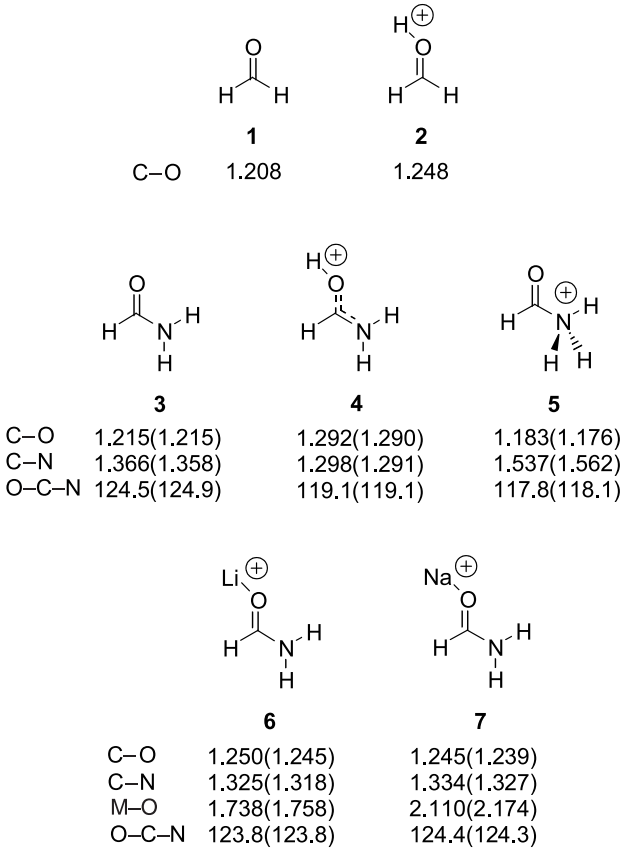

Fig. 1 Ground state structures used to calculate vertical excitation energies: experimental bond distances/ Å for **1** and **2**, data calculated by the MR-CISD/aug-cc-pVDZ (*MP*2/cc-pVTZ values in brackets) method for **3**–**7**

the *MP*2/6-31G* study of *Tortajada et al.* [24]. This finding, as stated earlier, reflects the fact that the interaction between formamide and the given metal monocations is essentially electrostatic with the ion-dipole interaction being the dominant term. Accordingly, structural changes associated with Li^+ and Na^+ cationization are expected to be smaller than in the case of protonation. Comparison of the optimized structures displayed in Fig. 1 corroborates this supposition. For instance, the C–O bond distance is elongated by 0.030 and 0.024 Å upon binding with Li^+ and Na^+, while O-protonation causes an increase of 0.075 Å (at the *MP*2/6-31G* level of theory). Similarly, the C–N bond becomes shorter by 0.040 (Li^+ complex) and 0.031 Å (Na^+ complex), as compared to 0.067 Å in the O-protonated species. The OCN valence angle remains practically unchanged upon complexation with the considered metal cations.

Calculation of vertical excitation energies of formaldehyde and formamide and their protonated forms

The vertical excitation energies of formaldehyde and its protonated form were calculated at three levels of theory: MCSCF, MR-CISD and MR-CISD + Q [4]. The +Q indicates the use of the *Davidson* correction. All methods used in this work are described in detail in Ref. [5]. Here, we shall focus only on the differences between their electronic spectra, based on the results obtained by the MR-CISD + Q method. They are summarized in Fig. 2 and Table 1. Analysis of the calculated vertical ionization energies for formaldehyde reveals (see Fig. 2) that the lowest singlet state corresponds to the 1^1A_2 (n_O–π^*) state followed by a series of *Rydberg* states and the 1^1B_1(σ_{CO}–π^*) and 3^1A_1(π–π^*) valence states. The π–π^* transition is the one with the largest intensity as expected. Protonation of formaldehyde causes significant changes in the excitation spectrum. In particular, the n_O–π^* state, as well as the *Rydberg* states, appear to be significantly shifted toward higher energies. On the other hand the π–π^* and σ_{CH}–π^* states remain almost unchanged. As a consequence, the lowest three bands in the spectrum correspond to valence states. They are followed by *Rydberg* states and the σ_{CO}–π^* and $n_O{}^0-\pi^{*2}$ valence states [4].

The UV spectra of formamide and its N- and O-protonated forms, using the MR-CISD and MR-CISD + Q methods have been described in detail in our previous work [5]. In carrying out the MR-CISD + Q calculations three different reference

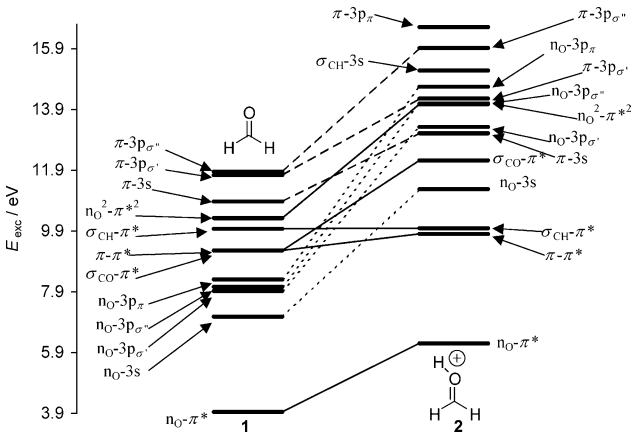

Fig. 2 Comparison of the calculated electronic excitation energies/eV of formaldehyde and protonated formaldehyde at MR-CISD + Q level

Table 1 MR-CISD + Q/d′-aug-cc-pVDZ calculated vertical excitation energies/eV for valence and *Rydberg* excited states of structures **1**–**7**. MR-CISD/d′-aug-cc-pVDZ calculated oscillator strengths are given in parentheses[a]

State	**1**	**2**	**3**	**4**	**5**	**6**	**7**
$n_O-\pi^*$	3.95 (0.000)	6.20 (0.001)	5.78 (0.001)	9.01 (0.000)	5.18 (0.000)	6.54 (0.000)	6.36 (0.001)
$\pi-\pi^*$	9.35 (0.116)	9.80 (0.240)	7.71 (0.338)	7.83 (0.354)	10.73 (0.305)	7.41 (0.293)	7.42 (0.296)
$\sigma_{CO}-\pi^*$	9.26 (0.001)	12.22 (0.014)					
$\sigma_{CH}-\pi^*$	9.97 (0.000)	9.99 (0.001)					
$n_O{}^2-\pi^{*2}$	10.33 (0.015)	14.07 (0.004)					
$\pi_b-\pi^*$				11.16 (0.062)			
n_O-3s	7.08 (0.025)	11.28 (0.003)	6.78 (0.006)	11.81 (0.048)	8.87 (0.050)	8.06 (0.102)	7.50 (0.009)
$n_O-3p_{\sigma'}$	7.93 (0.040)	13.33 (0.138)	7.47 (0.058)	13.03 (0.039)	9.63 (0.067)	9.39 (0.069)	
$n_O-3p_{\sigma''}$	8.06 (0.050)	14.10 (0.093)	7.84 (0.017)		10.43 (0.060)	9.31 (0.078)	8.86 (0.110)
n_O-3p_{π}	8.30 (0.000)	14.65 (0.001)	8.08 (0.013)		10.73 (0.023)	9.62 (0.001)	9.27 (0.001)
$\pi-3s$	10.87 (0.041)	13.12 (0.039)	6.77 (0.021)	9.52 (0.007)	12.02 (0.005)	7.95 (0.001)	7.50 (0.001)
$\pi-3p_{\sigma'}$	11.74 (0.029)	15.26 (0.013)	7.62 (0.000)	10.22 (0.025)	12.79 (0.000)	8.75 (0.027)	8.41 (0.020)
$\pi-3p_{\sigma''}$	11.85 (0.000)	15.93 (0.028)	8.03 (0.001)	10.88 (0.000)		9.12 (0.000)	
$\pi-3p_{\pi}$		16.61 (0.005)	8.28 (0.033)	12.03 (0.021)		9.80 (0.016)	9.37 (0.003)

[a] Experimental and calculated *MP*2/cc-pVTZ ground state geometries were used for **1**, **2** and **3**–**7** structures, respectively. The lithium and sodium atoms were described by a cc-pVDZ basis. The complete active space (CAS) comprised 8 orbitals and 10 electrons, while the CI reference space included 6 orbitals and 8 electrons for **3**–**7**. A CAS with 6 orbitals and 8 electrons was used for **1** and **2**. *Rydberg* excitations were described by using an AUX space with 3s and 3p *Rydberg* orbitals

spaces had been used. In the following, all excitation energies discussed refer to the calculation with the intermediate reference space (comprising of 6 orbitals and 8 electrons) if not specified otherwise. For a more detailed discussion we refer to Ref. [5]. The calculated vertical excitation energies for the studied species at this level of theory are displayed in Fig. 3

Survey of the results presented in Fig. 3 shows that the calculated electronic absorption spectrum for O-protonated formamide differs considerably from that of the neutral molecule. The first band

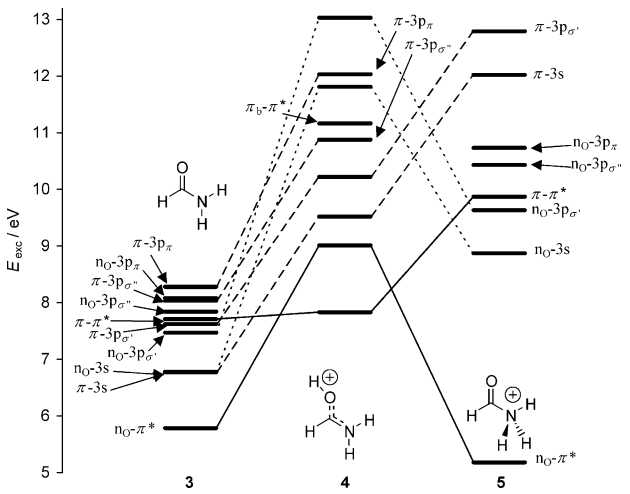

Fig. 3 Comparison of the calculated electronic excitation energies/eV of **3**, **4** and **5** at MR-CISD + Q level of theory

corresponds to the $\pi-\pi^*$ state (which remains almost unchanged as compared to that in the neutral molecule), whereas the $n_O-\pi^*$ valence state is shifted by ~3.2 eV to higher energies and appears as the second excited state. Such a strong increase in excitation energy of the $n_O-\pi^*$ state is due to a strong interaction of the n_O orbital with the proton. Furthermore, in contrast to the parent molecule, the typical valence-*Rydberg* mixing found in formamide was not present due to a shift of *Rydberg* states by more than 2.5 eV to higher excitation energies. This, as shown earlier, resembles closely the trend observed on going from the neutral to the protonated formaldehyde. More specifically, while in the parent formaldehyde the $\pi-\pi^*$ state is completely embedded in *Rydberg* states, in the protonated formaldehyde this state is located about 1.50 eV below the first *Rydberg* (n_O-3s) state [4]. It is also interesting to note at this point that upon protonation the $n_O-\pi^*$ valence state in formaldehyde undergoes a less pronounced shift to higher energy (by ca. 1 eV) than in formamide. Finally, a new $\pi-\pi^*$ valence state (denoted as $\pi_b-\pi^*$ valence state in Fig. 3) appears with an excitation energy of 11.16 eV.

Contrary to the electronic spectrum of the O-protonated form, the calculated UV spectrum of its N-protonated counterpart resembles more closely characteristic features of the spectrum of the neutral molecule. For instance, the lowest excited state is the

n_O–π^* state which is found at lower excitation energy than in the neutral molecule by about 0.6 eV. Furthermore, as in the parent molecule, the π–π^* valence state appears to be embedded into the region of *Rydberg* states and mixed strongly with them. It has a considerably larger excitation energy (10.73 eV) than for the neutral molecule (7.71 eV). The *Rydberg* states are also moved by several eV to higher excitation energies, with the shift of the π–*Ryd* states being significantly more pronounced.

Calculation of vertical excitation energies of formamide and its adducts with Li^+ and Na^+ cations

Metal cation association of formamide can in principle lead to the formation of three structurally different complexes: N-cationized, O-cationized and bidentate complex. As shown earlier, based on DFT and *MP*2 calculations [24–28], association with Li^+ and Na^+ takes place exclusively at the oxygen atom. This fact was also verified at the MR-CISD level [22]. Therefore, for the sake of comparison of the calculated vertical excitation energies with those of the O-protonated formamide discussed in the previous section, we shall use *MP*2/cc-pVTZ optimized structures of the metal ion adducts (Fig. 1). Analysis of the calculated vertical excitation energies (Table 1) shows that the ordering of the two valence excited states for both metal ion complexes remains the same as in the parent molecule, but they move energetically closer together. Namely, while the n_O–π^* state is shifted to higher energies by 0.76 and 0.58 eV for Li^+- and Na^+-formamide, respectively, the excitation energy of the π–π^* state is found to be lower for both complexes by ca. 0.3 eV than in the neutral molecule.

Specifically, in case of Li^+-formamide the lowest excited state lies 6.54 eV above the ground state and has very small oscillator strength (0.0003) typical for this kind of transition. It is followed by the strongly allowed π–π^* transition with a calculated excitation energy of 7.41 eV and an oscillator strength of 0.293.

The two *Rydberg* series, π–*Ryd* and n_O–*Ryd*, start with π–3s and n_O–3s transitions at 7.95 and 8.06 eV. In the energy region above 8 eV, the n_O–*Ryd* states dominate the electronic spectrum due to larger oscillator strengths as compared to the π–*Ryd* states. The only exception is provided by the $3p_\pi$ states where the n_O–$3p_\pi$ state possesses a rather low oscillator strength of 0.0008.

In the Na^+ adduct the n_O–π^* and π–π^* states have excitation energies of 6.36 eV and 7.42 eV. Transition from the ground state to the latter state is the most intense transition in the spectrum (f = 0.296). In the vicinity of this state, a pair of *Rydberg* 3s states at 7.50 eV originating from the n_O and π excitations is found. Electronic excitation from the n_O and π orbitals into *Rydberg* 3p orbitals produces a series of states which starts with the π–$3p_{\sigma'}$ state with an excitation energy of 8.41 eV. The manifold of these *Rydberg* 3p excited states shows only minor differences with respect to the Li^+-formamide complex.

Adiabatic excitation energies of formamide and its protonated forms

To gain insight into the effect of geometry relaxation upon photoexcitation of formamide and its protonated forms we optimized the geometries of all considered species in the first excited state. Optimization of geometries of formamide and its protonated forms was carried out at the MR-CISD level [5]. The resulting minimum energy structures are shown in Fig. 4. Total electronic energies and adiabatic excitation energies for structures **8**–**11** calculated at the same level of theory have been collected in Table 2.

Before analysing changes in the excitation energies upon geometry relaxation we shall describe

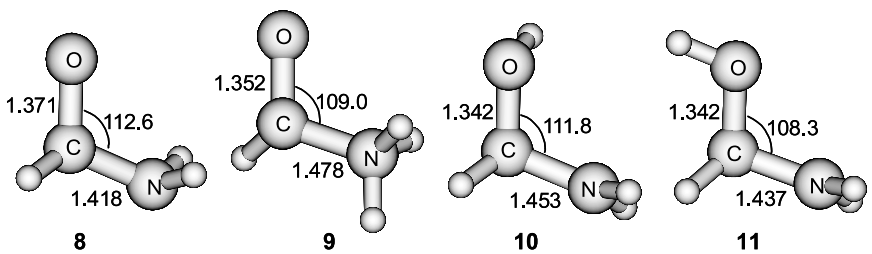

Fig. 4 MR-CISD optimized geometry parameters of structures **8**–**11** in the first excited state. Bond lengths are in Ångstrøms and bond angles in degrees

Table 2 Calculated total (E_{tot}/a.u.) and adiabatic excitation energies (E_{exc}/eV) for structures **8**–**11** at MR-CISD + Q level of theory[a]

	8	**9**	**10**	**11**
E_{tot}	−169.33147 (−169.45744)	−169.65122 (−169.78125)	−169.65539 (−169.78353)	−169.66045 (−169.78862)
E_{exc}	4.36 (4.47)	3.94 (4.02)	4.58 (4.72)	4.44 (4.58)

[a] Results in parentheses are calculated at the MR-CI + Q/aug'-cc-pVTZ level

geometrical features of the investigated species in the first excited state in some detail (Fig. 4). Comparison of the ground state geometries and the geometries in the first excited singlet state shows that the geometrical relaxation of formamide resulted in pronounced pyramidalization at the carbon and nitrogen atoms. This is expected from qualitative considerations and results from an increase of electron density on carbon relative to the ground state [29]. Both, the C–O and C–N bond distances become stretched by 0.16 and 0.05 Å. Their weakening is also reflected in the shift of harmonic vibrational frequencies of the CO and CN stretching modes (computed at the SA-CASSCF/aug-cc-pVDZ level) from 1800.3 and 1325.2 cm^{-1} in the ground state to 1061.4 and 1121.5 cm^{-1} in the excited state. The fact that the formamide geometry deviates from planarity compares well with previous calculations using the much simpler CIS/6-31G* method [29]. However, our calculations predict a significantly longer CO bond (1.371 Å) as compared to the CIS results (1.272 Å).

Similar to the parent molecule, the first excited singlet state of N-protonated formamide is characterized by a strongly pyramidalized carbon atom (see Fig. 4). Furthermore, a shortening of the CO bond by 0.019 Å and stretching of the CN bond by 0.060 is observed with respect to the excited-state formamide **8**. These trends, although less pronounced, are in accord with geometrical changes observed upon N-protonation in the ground state (−0.032 and 0.171 Å). It is also interesting to note that the orientation of the NH_3 group with respect to the CO bond in the excited state structure **9** is almost opposite to that in the ground state structure **5**. The dihedral angle O–C–N–H2 is 184.9° and 0.0° in excited and ground state, respectively.

For O-protonated formamide two structures, **10** and **11**, were found, with the latter being more stable by 13.3 kJ mol^{-1} (MR-CISD + Q). In both structures pyramidalization of the N-atom is negligible and the NH_2 group is found to be almost perpendicular to the O–C–N plane. Furthermore, shortening of the CO bond in **10** and **11** relative to the same bond in neutral formamide **8** is observed. On the other hand, the CN bond lengths are stretched relative to **8** (1.453 Å (**10**) and 1.437 Å (**11**) vs. 1.418 Å (**8**)). The stretching of the CN bond in **10** or **11** of about 0.15 Å is even more remarkable when compared to the ground state structure **4**. All these changes are indicative of a reduction of the conjugative interaction between the CO and the NH_2 groups.

The adiabatic excitation energies of formamide and its N- (**9**) and O-protonated structures (**10**, **11**) calculated with respect to the ground state of formamide (**3**), N- (**5**) and the lowest energy O-protonated form **4**, are summarized in Table 2. As expected from the large geometry relaxation effects, all adiabatic excitation energies differ considerably from the vertical ones. The largest effect is noted for the O-protonated form (E_{exc} (vert.) = 7.89 eV vs. E_{exc} (adiab.) = 4.44 eV). On the other hand, geometry relaxation in formamide and in N-protonated formamide has a smaller effect on the excitation energy and is of similar magnitude (1.3 and 1.4 eV, respectively), implying that the energy of the n_O–π^* state is less influenced by geometry relaxation than the π–π^* state is in O-protonated formamide. It is also worth mentioning at this point that geometry relaxation in formamide adducts with lithium and sodium cations has a less pronounced effect on the excitation energy (relaxation energies are 2.2 and 1.8 eV, in the Li^+ and Na^+ adducts, respectively as compared to 3.4 eV in the O-protonated formamide) of the lowest excited state [22].

Gas phase basicity and metal ion affinities of form-amide in the first excited state

The gas phase basicity, *GB*, of a base B is formally defined as the standard *Gibbs* free energy change (ΔG°) for the reaction given in Eq. (1), the corre-

Table 3 Standard reaction enthalpies, entropies and *Gibbs* free energies for protonation of formamide in ground and first excited state[a]

	ΔH°/kJ mol^{-1}	ΔS°/J mol^{-1} K^{-1}	ΔG°/kJ mol^{-1}
Ground state			
4	840.1 (822.2)[b]	118.8	805.0 (791.2)[b]
5	775.3	107.1	743.5
Excited state			
9	805.0	110.0	772.4
10	815.0	113.4	781.2
11	830.1	113.0	796.2

[a] Total energies taken from MR-CI + Q calculations; *ZPVE*, T_c and S° taken from *MP*2/aug-cc-pVDZ and CASSCF/aug-cc-pVDZ calculations for ground and excited states. [b] Experimental values from Ref. [31]

sponding proton affinity, *PA*, being the standard enthalpy change (ΔH°) for the same reaction.

$$BH^+(g) \rightarrow B(g) + H^+ \quad (1)$$

GB and *PA* values were computed using standard thermodynamical procedures in the framework of the harmonic oscillator – rigid rotor ideal gas approximation. Total electronic energies E_{tot} for the optimized structures were taken from MR-CISD + Q calculations. For the entropy of the proton $S^\circ(H^+)$ the experimental value of 108.95 J mol^{-1}K^{-1} was taken from Ref. [30]. The calculated values of standard reaction enthalpies, entropies and *Gibbs* free energies are collected in Table 3 along with the corresponding data for the ground state protonation.

The gas-phase basicity and proton affinity of formamide have been determined experimentally [31] for the ground state allowing us to test the accuracy of our calculations in this case. The corresponding calculated values, related to protonation at the O-site are 805.0 and 840.1 kJ mol^{-1}, which is by 13.8 and 17.9 kJ mol^{-1} higher than the experimental values (791.2 and 822.2 kJ mol^{-1}) [31].

Analysis of the results in Table 3 obtained with the aug-cc-pVDZ basis shows that the oxygen basicity in formamide decreases upon excitation to the first excited state. Calculated *GB* and *PA* values for the excited state are 796.2 and 830.1 kJ mol^{-1}, respectively. On the contrary, the N-atom becomes more basic by 29 kJ mol^{-1} than in the ground state. Consequently, the strong preference for protonation at the O-atom in the ground state (62 kJ mol^{-1}) diminishes to only 24 kJ mol^{-1}.

Using a similar approach as outlined above, we have also calculated gas phase affinities and basicities of formamide towards lithium and sodium cation in the ground and in the first excited singlet state [22]. In this way the ground state metal ion affinities of 216.3 and 152.3 kJ mol^{-1} for the Li^+ and Na^+ adduct, were obtained. The corresponding metal ion basicities assume the values of 178.7 and 113.4 kJ mol^{-1}. It should be noted that the calculated lithium cation basicity is in quite good agreement with the experimentally [25] measured gas phase value at 373 K (156.8 kJ mol^{-1}). Upon electronic excitation, metal ion affinities, as well as the metal ion basicities, were found to decrease significantly, thus resembling a trend observed for the proton affinity and basicity of formamide. Specifically, the lithium cation affinity and basicity drop to 195.4 and 159.8 kJ mol^{-1}, respectively, while for sodium cation the corresponding values are 117.2 and 79.5 kJ mol^{-1}.

Photochemistry of formamide

Upon photo-excitation, there are five main channels of formamide dissociation: (1) C–N dissociation leading to formation of $NH_2 + CO + H$, (2) C–H dissociation to $NH_2CO + H$, (3) formation of H + NHCHO by N–H dissociation, (4) direct formation of NH_3 and CO, and (5) H_2 abstraction resulting in H_2 + HNCO. Experimental investigations in gas-phase [32] and in low temperature matrices of argon and xenon [33] have shown that the importance of each of these channels strongly depends on the specific environment effects.

In the gas phase, the major products observed after photodecomposition of formamide at 150°C are CO, NH_3, and H_2 with quantum yields of 0.8, 0.2, and 0.6 [32]. In solid Ar matrix, formamide photolysis after 193 nm (6.42 eV) absorption [33] has as main photo-dissociation channel the formation of a weakly bound $NH_3 \cdots CO$ complex. On the other hand, when formamide is trapped in a solid Xe matrix strong external heavy-atom effect induces intersystem crossing to the triplet state yielding HNCO + H_2 photo-products. A comprehensive theoretical study of photodissociation of formamide was published by *Fang* and coworkers [34], which used the CASPT2 method for the calculation of transition structures for C–N, C–H, and N–H dissociation in the first singlet and triplet states. It was shown that the lowest energy pathway in the first singlet excited

state and in the first triplet state is C–N bond breaking with an energy barrier of 82.4 kJ mol^{-1} (0.85 eV) and 56.1 kJ mol^{-1} (0.58 eV), respectively. It is interesting to mention that *Maier et al*. [35] as well as *Duvernay et al*. [36] studied the behavior of formamide upon iradiation with light of wavelengths 248 nm (5.00 eV) and 240 nm (5.17 eV), respectively, in solid matrices. Irradiation of formamide under these conditions led to the formation of formamidic acid, which is the simplest example of a photo induced hydrogen/proton transfer [37].

We have recently performed excited-state dynamics simulations for formamide in the gas phase, by employing the semi-classical direct trajectory with surface hopping method [38] implemented in the NEWTON-X program package [21]. State averaging CASSCF(10,8)/6-31G(d) over three singlet states have been applied for calculating excited state energies, gradients, and nonadiabatic transition probabilities. The dynamics calculations for 100 trajectories starting at the first excited singlet state have shown [39], in agreement with experiments, that the major process for decomposition is C–N dissociation (76% of trajectories) with a lifetime around 420 fs. In 15% of trajectories, formamide moves to the minimum of the excited state and remains trapped there without returning to the ground state within the simulation time (1000 fs). The formation of vibrationally hot formamide in the ground state was observed in 5% of the trajectories, while C–H dissociation appeared in 4% of them. No indication of excited state proton transfer in the first excited state PES was found. From a mechanistic point of view, the main process, CN dissociation, is triggered by a fast transfer of energy from the CO stretching mode to the CN stretching mode that takes place at about 400 fs (Fig. 5). The consequent elongation of the CN bond brings formamide to a conical intersection in which it returns to the ground state. More information on the photodynamics of formamide can be found in a separate publication [39].

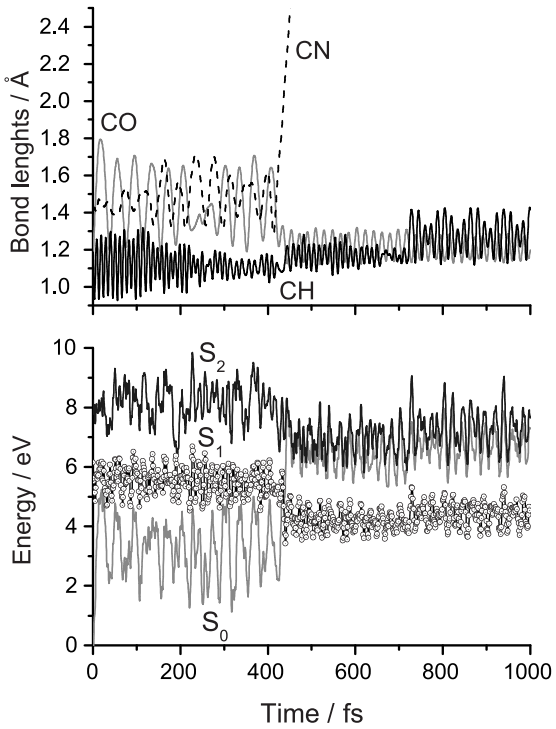

Fig. 5 Time evolution of C–O, C–N, and C–H bond lengths (top) and potential energies (bottom) of the ground and excited states of formamide in one selected trajectory of the most common type. The dots in the potential energy graph indicate the current state of the system in each time step

Conclusions

The vertical excited energies and oscillator strengths for singlet states of formaldehyde and formamide and their protonated forms, as well as of lithium and sodium cation complexes with formamide were calculated using the MR-CISD + Q approach, in order to elucidate the effect of cationization on the vertical electronic spectrum of formamide. The results show a significant effect of protonation on the computed UV absorption spectrum. Particular large effects were found for the O-protonated form where the n_O–π^* state is shifted strongly to higher energies and where the π–π^* state is now the lowest excited state. These changes closely resemble those found for protonated formaldehyde. On the other hand, the UV spectrum of the N-protonated form resembles more closely the spectrum of the neutral form. Complexation with Li^+ and Na^+ leads to a pronounced shift of the n_O–π^* state to higher energies while the π–π^* state moves in opposite direction by 0.3 eV. It is, however important to note that, in contrast to protonation, complexation of formamide by both metal cations does not effect the ordering of the first two lowest valence excited states, thus being at variance with the situation observed upon O-protonation.

Geometry optimizations in the lowest excited singlet show a pronounced pyramidalization of formamide both at the carbon and nitrogen atoms. The structure of N-protonated formamide in the first ex-

cited singlet state is also strongly pyramidalized at the carbon atom whereas the O-protonated form shows negligible N-pyramidalization in the excited state. Substantial energetic shifts of up to 3.4 eV have been observed due to geometry relaxation to the energy minimum for the protonated formamide. In comparison, for adducts of formamide with lithium and sodium cations much smaller changes were found. Calculated gas phase basicities show that the strong preference for protonation at the oxygen atom found for the ground state is strongly diminished in the excited state.

The photodynamical simulations on formamide show that the main primary deactivation path is CN dissociation with a lifetime of about 420 fs. No indication of excited state proton transfer in the first excited state was found.

Besides the presentation of an overview about the excited states of formamide and its derivatives, another more general goal of the current work was to show how high-level *ab initio* quantum chemical calculations based on multireference methods have become a powerful tool in the analysis of photoabsorption spectra, of photochemical and photophysical processes activated in the excited states, and of relaxation processes by which the system returns to the ground state either *via* photoemission or nonradiative pathways.

Acknowledgements

The authors acknowledge support by the WTZ treaty between Austria and Croatia (Project Nos. 9/2004/2006), the COST D37 action, and the Austrian Science fund within theframework of the Special Research Program F16 and project P18411-N19 (*H.L.* and *M.B.*). The work in Zagreb (*I.A.* and *M.E.M.*) has been supported by the Ministry of Science and Technology of Croatia through project 098-0982933-2920. The calculations were performed in part on the *Schrödinger* III Linux cluster of the Vienna University Computer Center.

References

1. Excited state proton transfer: a) Tolbert LM, Solntsev KM (2002) Acc Chem Res 35:19; b) Agmon N (2005) J Phys Chem A 109:13; c) Knochenmuss R, Fischer I (2002) Int J Mass Spectrom 220:343; d) Hynes JT, Tran-Thi T-H, Granucci G (2002) J Photochem Photobiol A Chem 154:3; e) Wan P, Shukla D (1993) Chem Rev 93:571; f) Martynov IY, Demyashkevich AB, Uzhinov BM, Kuzmin MG (1977) Uspekhi Khimii 46:3; g) Arnaut L, Formosinho SJ (1993) J Photochem Photobiol A 75:1
2. a) Formosinho SJ, Arnaut L (1993) J Photochem Photobiol A 75:21; b) Ormson SM, Brown RG (1994) Progr React Kinet 19:45; c) Douhal A, Lahmani F, Zewail AH (1996) Chem Phys 207:477; d) Crespo-Hernandez CE, Cohen B, Hare PM, Kohler B (2004) Chem Rev 104:1977; e) Legourrierec D, Ormson SM, Brown RG (1994) Progress React Kinetics 19:211
3. a) Scheiner S (2000) J Phys Chem 104:5898; b) Sobolewski AL, Domcke W (2006) Chem PhysChem 7:561; c) Cukier RI, Zhu JJ (1999) J Chem Phys 110:9587; d) Aquino AJA, Lischka H, Hättig C (2005) J Phys Chem A 109:3201; e) Cukier RI, Zhu JJ (1999) J Chem Phys 110:9587
4. Antol I, Eckert-Maksić M, Müller T, Dallos M, Lischka H (2003) Chem Phys Lett 374:587
5. Antol I, Eckert-Maksić M, Lischka H (2004) J Phys Chem A 108:10317
6. Moule DC, Walsh AD (1975) Chem Rev 75:67 and references therein
7. Gingell JM, Mason NJ, Zhao H, Walker IC, Siggel MRF (1997) Chem Phys 220:191 and references therein
8. Whitten JL, Hackmeyer M (1969) J Chem Phys 51:5584
9. Buenker RJ, Peyerinhoff SD (1970) J Chem Phys 53:1368
10. Basch H, Robin MB, Kuebler NA (1967) J Chem Phys 47:1202
11. Merchán M, Roos BO (1995) Theor Chim Acta 92:227
12. Serrano-Andrés L, Fülscher P (1996) J Am Chem Soc 118:12190
13. a) Yeager DL, McKoy V (1974) J Chem Phys 60:2714; b) Gwaltney SR, Rarlett RJ (1995) Chem Phys Lett 241:26
14. Szalay PG, Fogarasi G (1997) Chem Phys Lett 270:406
15. Hachey MRJ, Bruna PJ, Grein F (1995) J Phys Chem 99:8050
16. Müller T, Lischka H (2001) Theor Chem Acc 106:369
17. Müller T, Dallos M, Lischka H (1999) J Chem Phys 110:7176
18. Hirst JD, Hirst DM, Brooks CL III (1996) J Phys Chem 100:13487
19. a) Lischka H, Shepard R, Pitzer RM, Shavitt I, Dallos M, Müller T, Szalay PG, Seth M, Kedziora GS, Yabushita S, Zhang ZY (2001) PCCP 3:664; b) Lischka H, Shepard R, Brown FB, Shavitt I (1981) Int J Quantum Chem S 15:91; c) Lischka H, Shepard R, Shavitt I, Pitzer RM, Dallos M, Mueller T, Szalay PG, Brown FB, Ahlrichs R, Boehm HJ, Chang A, Comeau DC, Gdanitz R, Dachsel H, Ehrhardt C, Ernzerhof M, Hoechtl P, Irle S, Kedziora G, Kovar T, Parasuk V, Pepper MJM, Scharf P, Schiffer H, Schindler M, Schueler M, Seth M, Stahlberg EA, Zhao J-G, Yabushita S, Zhang Z, Barbatti M, Matsika S, Schuurmann M, Yarkony DR, Brozell SR, Beck EV, Blaudeau J-P (2006) COLUMBUS, an ab initio electronic structure program, release 5.9.1: www.univie.ac.at/columbus
20. a) Shepard R, Lischka H, Szalay PG, Kovar T, Ernzerhof M (1992) J Chem Phys 96:2085; b) Lischka H, Dallos M, Shepard R (2002) Mol Phys 100:1647; c) Dallos M, Lischka H, Shepard R, Yarkony DR, Szalay PG (2004) J Chem Phys 120:7330; d) Lischka H, Dallos M, Szalay PG, Yarkony DR, Shepard R (2004) J Chem Phys 120:7322

21. a) Barbatti M, Granucci G, Persico M, Ruckenbauer M, Vazdar M, Eckert-Maksić M, Lischka H (2007) J Photochem Photobio A Chem 190:228; b) Barbatti M, Granucci G, Ruckenbauer M, Persico M, Lischka H (2006) Newton-X: a package for Newtonian dynamics close to the crossing seam, v. 0.12b, www.univie.ac.at/newtonx
22. Antol I, Vazdar M, Eckert-Maksić M, Aquino AJA, Lischka H (2007) manuscript in preparation
23. Adhikari DD, Thakuria T, Medhi C (2000) Indian J Chem 39A:792
24. Tortajada J, Leon E, Morizur J-P, Luna A, Mó O, Yáñez M (1995) J Phys Chem 99:13890
25. Herreros M, Gal JF, Maria PC, Cecouzon M (1999) Eur Mass Spectrom 5:259
26. Tsang Y, Siu FM, Ho CS, Ma NL, Tsang CW (2004) Rapid Commun Mass Spectrom 18:345
27. Tsang Y, Siu FM, Ma NL, Tsang CW (2002) Rapid Commun Mass Spectrom 16:229
28. Remko M (1997) Mol Phys 91:929
29. Li Y, Garrell RL, Houk KN (1991) J Am Chem Soc 113:5895
30. Chase MW Jr (1998) NIST-JANAF Thermochemical Tables, 4th edn. J Phys Chem Ref Data Monograph 9:1–1951
31. Hunter EP, Lias SG (1998) J Phys Chem Ref Data 27:413
32. Boden JC, Back RA (1970) Trans Faraday Soc 66:175
33. Lundell J, Krajewska M, Räsänen M (1998) J Phys Chem A 102:6643
34. Liu D, Fang W-H, Fu X-Y (2000) Chem Phys Lett 318:291
35. Maier G, Endres J (2000) Eur J Org Chem 2000:1061
36. Duvernay F, Trivella A, Borget F, Coussan S, Aycard J-P, Chiavassa T (2005) J Phys Chem A 109:11155
37. Sobolewski AL (1995) J Photochem Photobiol A Chem 89:89
38. Tully J (1991) J Chem Phys 93:1061
39. Antol I, Eckert-Maksić M, Barbatti M, Lischka H (2007) J Chem Phys, in print